Advance Research in Textile Engineering

Open Access

Austin Publishing Group

Review Article

Systematic Investigation of The Multiphysical Characteristics of Silicon-Carbide Composites

Manyu Xiao[1*]; Zhiqin Chao[1]; Wenqing Zheng[1]; Xingang Luan[2]; Xinming Xu[2]; Weihong Zhang[3]

[1]School of Mathematics and Statistics, Northwestern Polytechnical University, Xi'an, 710021, China

[2]Science and Technology on Thermostructural Composite Materials Laboratory, Northwestern Polytechnical University, Xi'an, 710021, China

[3]School of Mechanical and Electrical Engineering, Northwestern Polytechnical University, Xi'an, 710021, China

***Corresponding author:** **Manyu Xiaoa**

School of Mathematics and Statistics, Northwestern Polytechnical University, Xi'an, 710021, China.

Email: manyuxiao@nwpu.edu.cn

Received: December 19, 2023

Accepted: February 14, 2024

Published: February 21, 2024

Abstract

With the exceptional properties of the low density, high strength and fracture toughness at high temperatures, fiber-reinforced matrix composites SiC_f/SiC are currently being applied for aircraft engine hot-section components. However, the oxidation and creep resistance of SiC_f/SiC still needs to be improved under complex service environments including simultaneously stress, high- temperature and atmosphere. This study employs a combination of experimental methods and data analysis techniques to accurately characterize and predict the damage and failure mechanisms, as well as the performance evolution of SiC_f/SiC in complex service environments. By utilizing performance data under different environments, a backpropagation neural network was used to characterize the influence of multi-field coupling on the mechanical performance. Additionally, an automatic construction of the oxidation kinetics model for SiC_f/SiC is developed with combination of both the physical model and available experimental data. The accuracy and effectiveness of models are experimentally verified for 2D and 3D composites.

Introduction

SiC fiber-reinforced SiC matrix composites(SiC_f/SiC)are considered to be promising materials for future systems operating in extreme thermal and mechanical environments, due to their excellent properties including high temperature resistance, lightweight, high strength, low thermal expansion, and oxidation resistance[1, 2]. Investigating the mechanical performance evolution and damage failure mechanisms of SiC_f/SiC in multi-field coupled service environments is important for material design, performance evaluation, and application[3]. However, due to the non- uniformity, nonlinearity, anisotropy, and diverse failure modes of SiC_f/SiC materials, their damage and failure mechanisms are complex. Currently, research efforts focus on the performance evolution of SiC_f/SiC composites in thermal-stress or thermal-oxygen environments through experimental means [4, 5], while the research on the coupled performance is still very limited. Indeed, the expensive experimental equipment and the complex oxidative test conditions at high temperatures lead to high costs for data acquisition, and the available data resources are limited. On the other hand, due to the complexity of the material, including the types of interface phases, matrix preparation methods, and fiber types, it is difficult to obtain relevant performance evolution laws [6, 7, 8, 9, 10].

Moreover, due to multiphase heterogeneity, anisotropy, multilevel porosity, and microcracks of SiC_f/SiC com- posites, as well as the influence of service environments, numerous factors affect high temperature mechanical prop-erties. Therefore, relying solely on experiments cannot meetthe urgent need for high temperature performance anal-ysis of SiC_f/SiC composites. Among theoretical models based on continuum damage mechanics (CDM) and micromechanics methods, Song Yingdong et al. [11] established a temperature-dependent constitutive model, well simulatingthe stress-strain curve of the material at room and high temperatures. Gao Xiguang et al.[12] established a constitu- tive model considering fiber bearing capacity and fracture, validated by experimental results, but not considering the effect of temperature [13]. In terms of micro-mechanics methods, Chen et al. [14] established a multi-scale progressive damage failure model for 2D woven SiC_f/SiC composites, using two damage variables to characterize the damage effects dominated by fibers and matrix, respectively. Anna Madra et al.[15] proposed a diffuse manifold learning based approach for constructing mesoscale geometric models of braided reinforcements in composites from X-ray micro- CT data to overcome ambiguities due to noise; At the sametime, they also devised a stochastic characterisation methodfor textile-reinforced com-

Citation: Xiao M, Chao Z, Zheng W, Luan X, Xu X, et al. Systematic Investigation of The Multiphysical Characteristics of Silicon. Adv Res Text Eng. 2024; 9(1): 1094.

posites based on X-ray microchro-matography scanning for assessing the uncertainty in the volume fraction of fibres in the composites[16].

However, the existing room temperature theoretical models cannot be directly applied to accurately charac- terize and predict the mechanical properties of SiC_f/SiC composites in multi-field coupled service environments. In terms of predicting the mechanical properties of composite materials (basic mechanical properties, constitutive relation- ships, fatigue performance), based on a large number of data obtained through experimental testing and numerical simulation, combined with artificial intelligence to mine the complex relationships between high-dimensional variables,fast response from parameters to performance can be achieved[17, 18]. For example, in terms of predicting basic mechanical properties, Sabiston et al. [19]used CT scanningto obtain cross-sectional images of composite materials at selected positions and characterized the fiber orientation us-ing a second-order tensor. They then built an artificial neural network to predict the fiber orientation tensor from positioncoordinates, and the trained artificial neural network can quickly and accurately predict the fiber orientation tensorat different positions of the molded composite material, laying a foundation for accurately predicting its mechanicalproperties. Anna Madra et al.[20] investigated a machine- learning based approach to determine the morphology and spatial distribution of defects in composites through X-ray micro-tomography. In terms of constitutive model construction, Zobeiry et al. [21]built an asymptotic damagemodel for laminated plates with quasilinearly connected artificial neural networks based on multi-level connectivity, and obtained load-POD (pin opening displacement) curves that were highly consistent with experimental results. In terms of fatigue performance prediction, Tao et al. [22] used neural networks with ordinary differential equations and β-variational autoencoders to model the stiffening degradationbehavior of fiber-reinforced composites and provided corre-sponding S-N curves. The prediction effect was significantly better than phenomenological models without the need to establish complex mechanical models.

In addition, artificial intelligence is widely used in mul-tiple fields [23] such as composite material structure opti- mization design and intelligent manufacturing. For example,in composite material optimization design [24, 25, 26], doesnot rely on designers' experience and intuition, and can automatically iterate and update design strategies to achieveglobal optimization or precise reverse design. In compositematerial manufacturing[27, 28], identifies the impact of various manufacturing parameters on mechanical proper- ties, improves manufacturing processes, and collaborates with precision robot systems to achieve new technologies for large complex structure forming. Also, in composite material health monitoring [29], artificial intelligence can associate multiple sensing signals with the relationship between composite material state and perform predictions and controls under complex loading conditions.

This study aims to analyze the influence of multiple coupling factors on the performance of SiC_f/SiC in high temperature complex environments. By combining exper- imental methods with intelligent data analysis techniques, and collecting data on the mechanical performance evo- lution of SiC_f/SiC materials in different environments, a numerical strategy based on machine learning is devel-oped to analyze the data and construct a kinetic multi-field coupled model for the oxidation of composite materials.

The goal is to comprehensively analyze the mechanical performance and evolution laws of SiC_f/SiC in multi-field coupled service environments, with a focus on improving oxidation resistance and creep performance.

The organization of this paper is as follows: Firstly,the paper introduces the method of constructing a pre-diction model for the mechanical performance parameters of SiC_f/SiC using the backpropagation neural network (BPNN) principle. This model aims to predict the mechan-ical properties of these materials based on their composi- tion and processing parameters. Next, the establishment of the oxidation kinetics model is emphasized. The proposed theoretical framework and method are developed to study the oxidation behavior of these materials under different conditions. Finally, the main findings and conclusions are summarized.

BPNN-based mechanical performance parameter prediction for SiC_f/SiC

This section, focues is on analyzing the influence of multiple coupled factors on the mechanical performance of SiC_f/SiC in complex environment by utilizing the mechan- ical performance evolution data under various environmentscombined with a numerical strategy based on machine learning methods.

2D SiC/SiC and 3D SiC/SiC are two different types of SiC/SiC composite materials. 2D SiC/SiC is a composite material prepared using domestic SiC fiber fabric as a preform with BN as the interfacial phase and $SiC\text{-}B_4C$ multilayer ceramics as the matrix. 2D SiC/SiC weaves the silicon carbide fiber into a two-dimensional orthogonal wo-ven fabric, which is then layered to form a two-dimensional fiber preform. On the other hand, 3D SiC/SiC is prepared using a three-dimensional four-directional method to create a three-dimensional fiber preform, with Hi-Nicalon silicon carbide as the toughening fiber. Additionally, SiC_f/SiC is a carbon-carbon composite material that incorporates con- tinuous silicon carbide reinforcement into a silicon carbide ceramic matrix, encompassing both 2D SiC/SiC and 3D SiC/SiC.

The data is collected from various individual environ- ments, including different temperatures, times, and atmo- spheres. The dynamic behavior curves of SiC_f/SiC, such as mass loss, elastic modulus, and residual strength, are fitted under distinct temperature, time, and atmosphere con-ditions. The objective is to analyze the impact of multiple coupled factors on the mechanical performance of SiC_f/SiCin complex environments utilizing machine learning meth- ods and the fitted curves.

As summarized in Table1, experimental data were col- lected for three aspects:

a) Elastic modulus of 2D SiC/SiC was measured at various temperatures and exposure times in a wet oxygen envi- ronment providing information on how the modulus of the material changes under different conditions;

b) Mass loss rates were determined when subjected to wet oxygen and argon environments for different durations;

c) Mass changes were measured under different temperatures and exposure times in an environments of

$P_{H_2O}:O_2:Ar = 14:8:78$kPa, $P_{H_2O}:O_2:Ar = 21:21:58$kPa, or in air.

Table 1: Fitting Cases.

Fitting type	Material type	Environment	Temperature (°C)	Fitting curve
Univariate fitting	2D SiC/SiC	Wet oxygen and argon	1300	Change of elastic modulus
		$PH_2O:O_2:Ar = 12:8:80kPa$	1300, 1200	Oxidation rate
		$PH_2O:O_2:Ar = 14:8:78kPa$	1000 - 1500	
Multivariable fitting	3D SiC/SiC	$PH_2O:O_2:Ar = 21:21:58kPa$	1000 - 1500	Mass change rate
		Air	1000 - 1400	

Table 2: BPNN training parameter setting.

Name	Layer	Neuron	Activation function	Loss function	Training objectives	Training set, Verification set and Test set
Univariate fitting	3	[1,8,1]	[Purelin, Logsig, Purelin]	Mean square	0.0001	60%: 20%: 20%
Multivariate fitting	3	[2,10,1]	[Purelin, Logsig, Purelin]	Loss function		

Data source and BPNN architecture

Data source

All the data used in this study were obtained through experiments conducted by the collaborative team of the superhigh temperature laboratory at Northwestern Poly- technical University. Using laboratory equipment, heat treatment experiments were conducted on SiC_f/SiC in a high-temperature tubular furnace, during which the weight change curve was recorded.

BPNN architecture

Backpropagation neural network (BPNN), as a type of artificial neural network (ANN), allows for the simulation of complex relationships among various factors [30].

As shown in Figure1, the BPNN model employed in thisstudy consists of three layers: the input layer, hidden layer, and output layer. During the propagation process, the elastic modulus and mass change of the SiC/SiC composite mate- rial are input signals at the input layer, processed through the hidden layer using the sigmoid activation function, and then passed to the output layer. The total error between the expected output and the actual values iign the output layer is calculated using the mean square loss function. By adjustingthe network weights and thresholds, the BPNN aims to approximate the desired output for the elastic modulus and mass change [31].

The choice of the number of layers in a neural net- work is usually based on the complexity of data fittingand task requirements. In this article's experimental data fitting, we chose a three-layer neural network due to the relatively simple data fitting relationship. Compared to a four-layer neural network, a three-layer neural network has the following advantages: Fewer parameters, easier training,reduced risk of overfitting, and improved generalization ability; Nonlinear activation functions (such as Sigmoid) enhance the network's expressive power and better fit nonlinear relationships; The regularization effect weakens in deep networks, while a three-layer network can better deal with overfitting problems. Therefore, a three-layer neural network was selected for data fitting in the experiment.

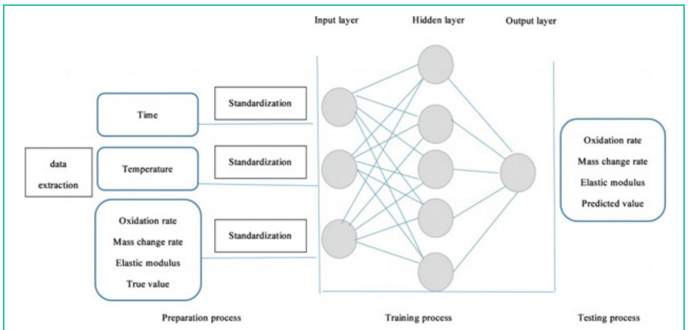

Figure 1: Back propagation neural network model.

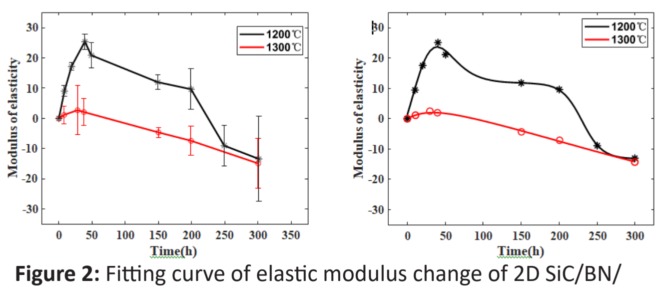

Figure 2: Fitting curve of elastic modulus change of 2D SiC/BN/SiC-B_4C materials with a self-healing matrix. a) Linear interpolation methods for fitting curves [32]. b) BPNN method for fitting curves.

Univariate fitting

Elastic modulus changes of 2D SiC/SiC composite materials in wet oxygen environment

To validate the BPNN, it was first used to test the uni- variate experimental data of 2D SiC/SiC composite materialshown in Figure 2(a), with the fitting curve obtained from the scatterplot of observed value points. When using the BPNN method to fit the elastic modulus change of 2D SiC/BN/SiC-B_4C materials, the experimentaldata is selected appropriately within the error range using the following equation:

As shown in Figure 3(a), the mean square errors for the training, validation, and testing sets are all less than 7.5008×10^{-4} after 211 iterations. The regression coefficient in Figure 3(b) is R=0.99789, indicating a good fit of the BPNN results. Additionally, the BPNN fitting curve in Figure 2(b) reveals important insights into the behavior of the 2D SiC/BN/SiC-B_4C under oxidation conditions. The elastic modulus initially increases, indicating improved mechanical properties. However, after oxidation, the modulus starts to decrease. This decrease is more pronounced at 1200°C and

$$(y_k)_{new} = (y_k)_{original} + \alpha \times \sigma \quad (1)$$

even faster at 1300°C, indicating a temperature dependent oxidation effect.

where $(y_k)_{original}$ is the average value of the original ex- perimental data,$(y_k)_{new}$ is the new data generated based on Eq.(1), α random number from a Gaussian distribution between 1 and -1, and σ represents the standard deviation ofthe experimental data.

The elastic modulus variation over time was fitted usingBPNN and ten data points were selected from Figure 2(a), corresponding to the red and black data points at 10, 20, 30, 40, 50, 100, 150, 200, 250, and 300 hours. The data set generated by Eq.(1) was used for neural network fitting.The BPNN fitting parameters were set as shown in Table 2.The fitting curve obtained using a 3-layer network is show in Figure 2(b), and the mean square error and regression analysis for evaluating the fitting results are shown in Figure 3.

Table 3: Mass change prediction of 3D SiC/SiC composites.

Environment	Number	Time (h)	Temperature (°C)	Mass change true value (%)	Mass change predicted value (%)	Relative error
$PH_2O: O_2: Ar = 14:8:78kPa$	1	4.138	1400	0.27218	0.2657	2.38%
	2	6.185	1300	0.2603	0.2641	1.46%
	3	8.1186	1200	0.1295	0.1286	0.69%
$PH_2O: O_2: Ar = 21:21:58kPa$	1	3.3777	1500	0.53643	0.5428	1.19%
	2	5.0666	1400	0.4603	0.4612	0.20%
	3	2.5333	1200	0.072471	0.0804	10.90%
Air	1	5.05	1400	0.03141	0.0322	2.52%
	2	8.35	1100	-0.0205	-0.0204	0.49%
	3	5.05	1000	-0.0541	-0.0542	0.18%

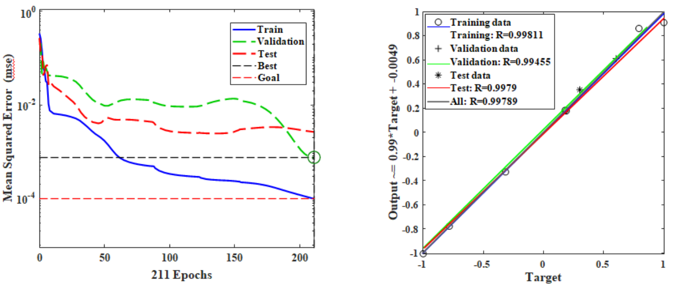

Figure 3: The mean square error diagram and regression analysis diagram by BPNN. a) Mean square error. b) Regression analysis.

Moreover, the comparison between the BPNN and the linear interpolation highlights the interest of the BPNN approach yielding a smoother variation of the elastic modulus over time in agreement with experimental results.

Oxidation rate of 2D SiC/SiC compositematerials in wet oxygen environment

To further verify the feasibility of BPNN for univariatefitting, we used BPNN to model the change relationship of the average mass loss rate per unit area of 2D SiC/BN/SiC-B_4C with time as shown in Figure 4(a), and compared it with the linear interpolation fitting method.

According to Figure 4(a), data points are sampled at10, 40, 50, 100, 150, 200, 250, and 300 hours in a wet oxygen environment, as well as black data points with ahorizontal axis of 10, 20, 40, 500, 100, 150, 200, 250,and 300 hours in an argon environment. The new data set generated by Eq.(1) was used for neural network fitting. The BPNN fitting parameters are set according to Table 2. The obtained fitting curve is shown in Figure 4(b). The mean square error and regression analysis for evaluating the fittingresults are shown in Figure 5.

As shown in Figure 5(a), after 285 iterations, the mean square error for the training set, validation set, and testing set are all less than 1.3666 × 10^{-3}. Furthermore, the regres- sion coefficient in Figure 5(b) is R=0.99636.

In summary, both the BPNN fitting curve and the con- ventional fitting curve in this study effectively capture the relationship between the unit area average mass change rate. However, the BPNN fitting curve appears smoother to represent the variation of the average mass change rate overtime.

Multivariable fitting

We primarily use BPNN to fit the mass change of 3D SiC/SiC under different time and temperature conditions

in an environments of $P_{H_2}O:O2:Ar$ = 14 : 8 : 78kPa, $P_{H_2}O:O2:Ar$ = 21 : 21 : 58kPa and air respectively. Theexperimental data in Figure 6 is utilized to analyze the mass

change at different times and temperatures.

Mass variation of 3D SiC/SiC under

$P_{H_2}O:O2:Ar$

= 14 : 8 : 78kPa ***environment***

We extracted the mass change values of 3D SiC/SiC in

$P_{H_2}O:O2:Ar$ = 14 : 8 : 78kPa environment from Figure 6, specifically within the time range of 0-10 hours and temperature range of 1000°C-1500°C. The BPNN method was employed to analyze the mass change pattern under different times and temperatures. The setting of BPNNfitting parameters

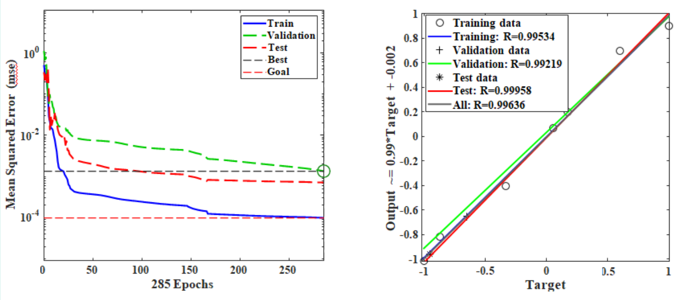

Figure 5: The mean square error diagram and regression analysis diagram by BPNN. a) Mean square error. b) Regression analysis.

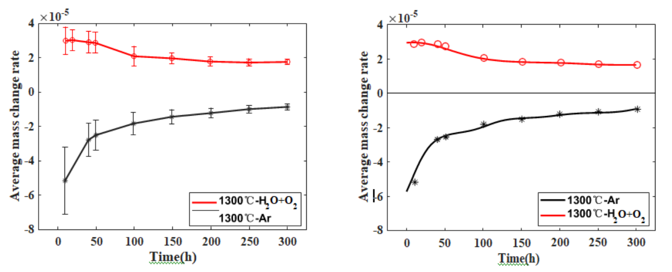

Figure 4: Fitting curve of oxidation rate in argon of 2D SiC/BN/SiC-B4C materials with a self-healing matrix. a) Linear interpolation methods for fitting curves [32]. b) BPNN method for fitting curves.

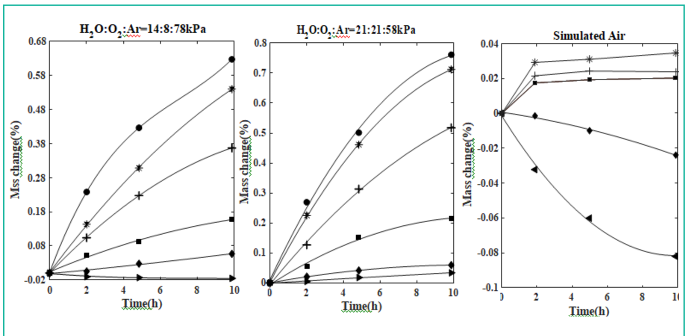

Figure 6: Fitting data source [33].

is given in Table 2,The evolution of the mean squared error is presented in Figure 7(a), the epochs represent the number of iterations, the regression analysis is displayed in Figure 8(a), and the fitting surface is shown in Figure 9(a).

From Figure 7(a), we can observe that after 1246 itera- tions, the mean square error for the training set, validation set, and testing set is less than 8.518×10^{-4}, with a satisfactory regression coefficient value of R=0.9941.

To ensure the reliability of the fitting results and avoid overfitting of the BPNN, several randomly selected points were tested against the neural network fitting curve, as givenin Table 3.

The predicted results indicate small errors between the actual and predicted values of mass change in the 3D SiC/SiC. This suggests that fitting by BPNN can effecti vely reflect the relationships among various multivariable fac- tors.

From the BPNN, graph in Figure 9(a), it can be ob- served that when the temperature is 1100°C, due to the lowtemperature (temperatures range from 1000°C– 1500°C, so 1100°C is considered relatively low), the oxidation productsof B_4C evaporate, resulting in slight mass loss of the mate- rial. However, as the reaction time prolongs, SiC is oxidized into SiO sealing defects, preventing B_4C from reacting with water and oxygen to become meteorological B_2O_3 andvolatilizing. Therefore, at lower temperatures (1000°C and 1100°C), the quality change of the material is controlled bythe chemical reaction rate, and its evolution

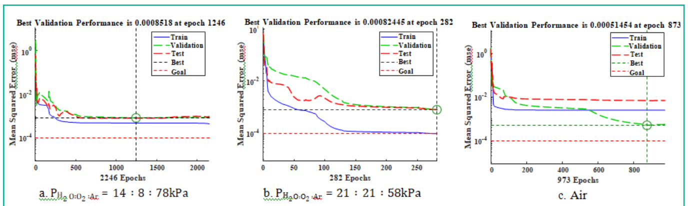

Figure 7: The mean square error diagram by BPNN.

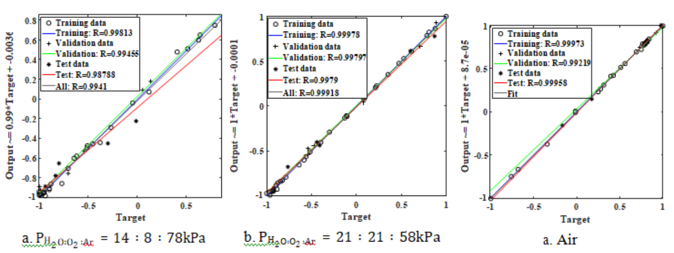

Figure 8: The regression analysis diagram by BPNN.

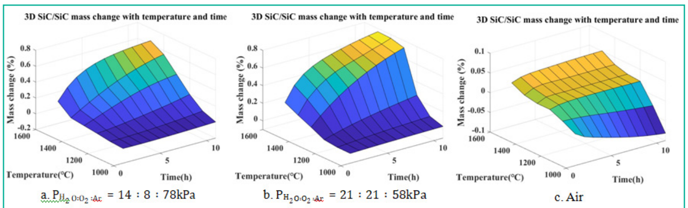

Figure 9: Mass fitting results of 3D SiC/SiC composites in different environments.

is linear. As thetemperature increases from 1200°C to 1500°C, the reactionrate of oxidation of SiC to SiO gradually increases, leadingto the quality change of the material being controlled by thediffusion rate in a wet oxygen atmosphere. Therefore, the quality change curve follows a parabolic growth pattern.

Mass variation of 3D SiC/SiC under

$P_{H_2}O{:}O_2{:}Ar$

= 21 : 21 : 58kPa ***environment***

In an environment of $P_{H_2}O{:}O_2{:}Ar$ = 21 : 21 : 58kPa, we extracted the mass change values of the 3D SiC/SiC from Figure 6. The temperatures ranged from 1000°C to

1500°C and the time intervals were from 0 to 10 hours. The BPNN parameters were determined based on Table 2. The evolution of the mean squared error is presented in Figure 7(b), the epochs represent the number of iterations, the regression analysis is displayed in Figure 8(b), and the fitting surface is shown in Figure 9(b).

As shown in Figure 7(b), after 282 iterations, the mean square error for the training set, validation set, and test set is less than 8.2445×10^{-4}, and the regression coefficient value R=0.99918. To validate the reliability of the results and check for overfitting, we randomly select several data points. Table 3 shows small errors between the actual and the predicted values of the mass change in the 3D SiC/SiC. This indicates that BPNN effectively captures mutual influ-ence patterns of various variables.

From Figure 9(b), it can be observed that between 1000°C and 1100°C, the mass change of the 3D SiC/SiC shows minimal variation over time. This is because at lowertemperatures, the oxidation rate of SiC/SiC is low, and the material's quality change is primarily controlled by chemi-cal reaction rates. On the other hand, at 1200°C, 1300°C, 1400°C, and 1500°C, respectively, the mass change con- tinuously increases over time. This is due to the faster generation of SiO_2 oxide layer above 1200°C, which resultsin the material's quality change being controlled by the reaction rate.

Mass variation of 3D SiC/SiC in different temperatures and times in air environment

We obtained the mass change values of the 3D SiC/SiCin the air environment from Figure 6, covering a time rangeof 0-10 hours and a temperature range of 1000°C– 1400°C.

The BPNN parameters are displayed in Table 2, the mean squared error can be observed in Figure 7(c),the regression analysis fitted surface in Figure 8(c), and finally, followed by the fitted surface in Figure 9(c) .

As shown in Figure 7(c), after 873 iterations, the mean square error of the training set, verification set and test setisless than 5.1454×10^{-4}, and the regression coefficient value R=0.99965.

Table 4: Data description of SiCf/SiC composite material model construction.

Material type	Environment	Temperature (°C)	Model
2D SiC/BN/SiC-B_4C	$PH_2O{:}O_2{:}Ar = 12:8:80$kPa	1300	Expression for the relationship between mass change and service time
		1200	
	$PH_2O{:}O_2{:}Ar = 21:21:58$kPa	1000, 1100, 1200, 1300, 1400, 1500	
3D SiC/SiC	$PH_2O{:}O_2{:}Ar = 21:21:58$kPa	1000-1500	Expression for the relationship between mass change, service time, and service temperature
	$PH_2O{:}O_2{:}Ar = 14:7:78$kPa		
	Air		

Table 5: Experimental data of the mass of 2D SiC/BN/SiC-B_4C composite material over time.

1300°C	Time (h) Mass change (%)	0	10.41	20.13	30.55	39.58	50.00	100.6	149.3	199.3	251.4	300.7
		0	0.056	0.171	0.341	0.473	0.525	0.761	1.129	1.504	1.693	1.967
1200°C	Time (h) Mass change (%)	0	11.08	20.78	29.79	40.18	49.88	99.77	150.3	200.2	249.4	300.0
		0	0.217	0.417	0.600	0.8217	0.913	1.461	1.996	2.517	3.052	3.600

Table 6: Parameter settings required for solving the 2D SiC/BN/SiC-B_4C and SiC/SiC composite material mode.

Material type	Temperature (°C)	Data classification	Data normalizaion
2D SiC/BN/SiC-B_4C	1300	Training Set: Test Set 80%: 20%	Score standardization
	1200		
3D SiC/SiC	1100		
Error function	Error function	Initial parameter value	Maximum number of iterations
Mean square Loss function	Mean square Loss function	[1,-0.5,1.8,1,-1,1]	10000
		[1,-1,2,1,-1.2,1]	
		[1,1,1.8,1,-1,1]	5000

Similarly, to verify the reliability of the results and check for overfitting, several points were randomly selected. The predicted results in Table 3 show small error between the actual and predicted values of the mass change.

From the diagram of BPNN in Figure 9(c), it can be seen that in the early stage of oxidation, due to the volatilization of B_4C oxidation products, the quality of SiC/SiC decreases. With the extension of oxidation time and the increase of temperature, its quality gradually increases. However, due to the absence of water in the air environment, the quality change of the material is only controlled by the diffusion rate of oxygen, so quality does not increase as much as in the water-oxygen environment.

In addition, the fitting and prediction of the quality change of 3D SiC/SiC under different environments reflect the influence of humidity on the quality of the material.

From dry air to $P_{H_2O:O_2:Ar} = 21 : 21 : 58kPa$, the water vapor pressure increases from 0 to 21%. At 1000°C and 1100°C and water vapor pressure of 0, some B_2O_3 and N_2 products are formed due to the reaction between BN and O_2, resulting in slight weight loss of the samples. However, when the water vapor pressure increases to 21% at low temperatures, SiC reacts with H_2O to generate SiO_2, and the weight gain of SiO_2 masks the weight loss caused by the reaction between O_2 and BN, resulting in an increase in the weight gain rate of the samples. As the temperature increases to 1200°C – 1400°C, at zero partial pressure, the material under goes a weight gain process. The weight gain rate is significant in the first 2 hours, but becomes very small after 2 hours. This is because the initial oxidation stage is controlled by chemical reactions and is temperature-dependent. A higher temperature leads to a faster reaction rate, resulting in a higher weight gain rate. As the reaction proceeds, SiO_2 is continuously formed, which acts as a barrier to prevent the contact between O_2 and the additives, leading to a decrease in the weight gain rate. Therefore, the change in material quality over time follows a parabolic pattern. When a water vapor pressure of 21% is added, the rate of reaction between H_2O and SiC generating SiO_2 significantly increases. Furthermore, water vapor has a stronger ability to penetrate the silica layer compared to oxygen, resulting in a noticeably higher weight gain rate compared to when the water vapor pressure is 0. Therefore, the parabolic pattern formed by the change in material quality over time becomes steeper.

In this section, an analysis of a neural network-based numerical data fitting method was conducted to extract its parameter characteristics from experimental data. When the training data is limited, the neural network outperforms conventional data fitting methods in single-variable fitting. For multivariable fitting, the reconstructed curves obtained using the neural network not only reflect the direct influence of temperature and time on the mass change of SiC/SiC composite materials but also provide good predictions for critical points. Furthermore, similar effects have been observed for external factors such as temperature, time, and atmosphere on the mass, elastic modulus, and strength of SiC/SiC composite materials.

Construction of the SiC_f/SiC composite material oxidation kinetics model

This section focuses on constructing the oxidation kinetics model of SiC_f/SiC under a multifield-coupled environment. Firstly, the method for predicting unknown parameters in the kinetic model is presented. Then, the initial architecture of the oxidation kinetics model for SiC_f/SiC under a multifield-coupled environment is established. Finally, based on the method for predicting unknown parameters, the constructed oxidation kinetics model is adjusted using experimental data. The specific contents are summarized in Table 4 which include the expression indicating the relationship between the mass change and service time for:

a) 2D SiC/BN/SiC-B_4C under high-temperature oxidation in a wet oxygen environment (at 1300°C and 1200°C, respectively).

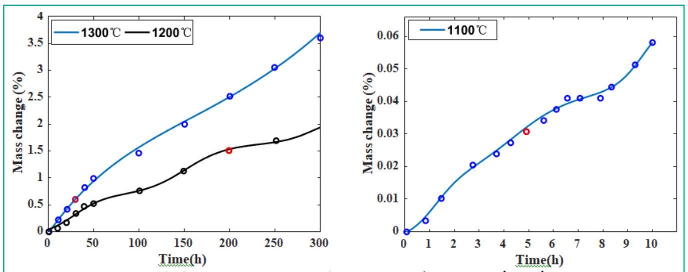

Figure 10: Model construction diagram. a) 2D SiC/BN/SiC-B_4C composite material at 1200°C and 1300°C. b) 3D SiC/SiC composite material at 1100°C

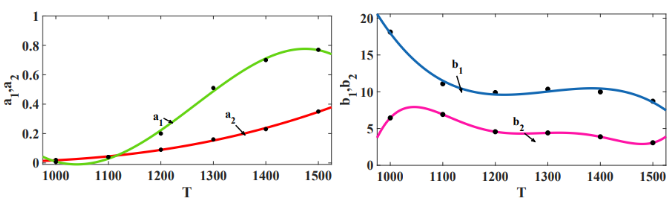

Figure 11: Fitting diagram of the relationship between a_1, a_2, b_1, b_2 and temperature ***T***. a) Fitting curve a_1, and a_2 with respect to the temperature ***T***. b) Fitting curve b_1 and b_2 with respect to the temperature ***T***.

b) 3D SiC/SiC under high-temperature oxidation in a wet oxygen environment.

c) 3D SiC/SiC under high-temperature oxidation in different environments, including $PH_2O: O_{2:Ar} = 14:8$: data preparation, model definition, loss function definition, selection of optimization algorithms, and parameter prediction. The selection of data classification, feature standardization, loss function, and optimization algorithm can significantly affect the prediction results of the model, and therefore, reasonable choices should be made based on the specific problem.

Two-dimensional oxidation kinetics model for

SiC_f/SiC

The two-dimensional oxidation kinetics model for SiC_f

/SiC is established to express the relationship between the material's mechanical property parameters and service time involving two steps: the initial architecture of theoxidation kinetics model and the determination of unknown parameters and model adjustment based on experimental data.

Existing oxidation kinetics models of SiC_f/SiC, constructed based on factor analysis methods, are derived froman extension of exponential functions [34]. In this section numerical simulation of SiC_f/SiC with BPNN, using the sigmoid activation function, which is the reciprocal form of the exponential function. This suggests that various factorsinfluencing the internal mechanisms of SiC_f/SiC (such as time, temperature, and mechanical property parameters) arelikely to follow the form of exponential functions.

Gaussian functions are a special form of exponential functions and are widely used to simulate various natural phenomena in the fields of natural science, engineering, andsocial sciences. For example, Gaussian functions can be used in the kinetic studies of chemical reactions to calculate the relative energy differences between reactants and products and predict reaction rates and pathways [35]. In chemistry, Gaussian functions can be employed to representthe electron density, predicting the interaction between drugmolecules and receptor molecules [36]. The changes in the mechanical properties of SiC_f/SiC under high-temperature 78kPa, $P_{H_2}O: O_2: Ar = 21: 21: 58$kPa, and air.

Estimation of unknown parameters of the model

When the initial architecture of the model is known, approximation algorithms such as moving least squaresand nonlinear least squares are commonly used to solvefor the unknown parameters. The specific process involves oxidation in different environments are, in fact, the result of interactions between various molecules, elements, and compounds.

Based on the above considerations, Gaussian functions are selected as the initial architecture of the oxidation kinetics model for SiC_f/SiC in a multifield-coupled environment. Using experimental data, it was found that the combination of two Gaussian functions can effectively represent the reaction behavior. Thus, the specific expression of the relationship between material mechanical properties and service time in a complex multifield-coupled environment isproposed as follows:

2.1×10^{-3}, which shows that the prediction results of model parameters are highly accurate.

To verify overfitting, we tested the model using data

with a service time of 29.79 hours. The model predicted a

$$y(t) = a_1 e^{-\left[\frac{(t-b_1)}{c_1}\right]^2} + a_2 e^{-\left[\frac{(t-b_2)}{c_2}\right]^2} \quad (2)$$

mass change value of 0.6076, with a small error of 0.0076 compared to the observed value of 0.6 further certifying the where y represents mechanical property parameters such asmass, stress, strength and modulus of SiC_f/SiC composites, t represents high temperature oxidation service time,

a_1, b_1, c_1, a_2, b_2 and c_2 are parameters to be identified.

In this section, 2D SiC/BN/SiC-B_4C composite is takenas an example, and its mechanical properties evolutiondata is used to construct the expression of the relationship between the mechanical properties, parameters and servicetime of 2D SiC/BN/SiC-B_4C composite.

Relationship between mass change and servicetime of 2D SiC/BN/SiC-B_4C at 1300 ˚C

The parameters are identified in the Eq.(2) of the relationship between mass change and service time of 2D SiC/BN/SiC-B_4C composites after high temperature oxidation at 1300°C under wet oxygen environment. The experimental data are shown in Table 5 , and the correspond-ing parameter settings are given in Table 6 . The valuesof a_1, b_1, c_1, a_2, b_2 and c_2 are obtained by as optimization accuracy of the predicted value of the model parameters. From Figure 10 (a), we can observe that all experimentaldata denoted with dot points are well distributed alongthe fitting curve figured with proposed model, indicating that the model effectively captures the relationship between mass change and service time of 2D SiC/BN/SiC-B_4C com-posites subjected to oxidation at 1300°C in a wet oxygen environment.

Relationship model between mass change andservice time of 2D SiC/BN/SiC-B_4C at 1200 ˚C

According to the methodology introduced in Section 3.1, we consider experimental data (Table 5) and the parameters (Table 6). Similarly, a_1, b_1, c_1, a_2, b_2 and c_2 are identified as the mass changes over time after oxidation ina wet oxygen environment 2D SiC/BN/SiC-B_4C at 1200°C shown in Table 7. The values of a_1, b_1, c_1, a_2, b_2 and c_2 are shown in Table 7, and the final expression of

Table 7: Predicted parameters of 2D SiC/BN/SiC-B_4C and 3C SiC/SiC composite material model.

Material Type	Temperature (°C)	a1	b1	c1	a2	b2	c2	Goodness of fit R2	Mean squared error
2D SiC/BN/SiC-B_4C	1300	1.893	2.2126	1.5271	-4.808	-2.6266	1.3889	0.9800	0.0021
	1200	1.744	1.7243	-1.1618	-1.202	-1.0958	0.5314	0.9701	0.0123
3D SiC/SiC	1500	0.77	8.71	4.85	0.35	3.06	2.1	0.98	0.04
	1400	0.7	9.98	5.04	0.23	3.87	2.67	0.99	0.02
	1300	0.51	10.34	4.86	0.16	4.4	2.9	0.99	0.013
	1200	0.2	9.88	4.47	0.09	4.56	2.6	0.965	0.006
	1100	0.04	11.08	2.07	0.04	6.91	4.44	0.99	0.002
	1000	0.007	18.11	7.34	0.02	6.44	3.1	0.95	0.002

Table 8: Parameter settings required for solving the 3D SiC/SiC composite material model.

Environment	Data classification	Data normalization	Error function
PH_2O: O_2: Ar = 21 : 21 : 58kPa	Training Set: Test Set 80%: 20%	Score standardization	Mean square Loss function
PH_2O: O_2: Ar = 14 : 8: 78kPa			
Air			
Optimization	**Initial parameter value**		**Maximum number of iterations**
Nonlinear Least Squares	[1,-0.5,1.8,-1.2,1,5,1,1,1,2,1,1,]		10000
	[3,1,5,1,16,1,1,1,1,10,1,1,10,1,-0.5]		5000
	[1,1,1,-1,-1,1,1,1,1,1,1,2,1,1,]		10000

the model is asfollows: algorithm, as shown in Table 7, and the model is: $-[\ (t-1.7243)\ ]^2 - [\ (t+1.0958)\ ]^2 - [\ (t-2.2126)\ ]^2\ [\ (t-2.6266)\ ]^2$ $y(t) = 1.744 \times -1.1618 - 1.202 \times e\ 0.5314$ (4) $y(t) = 1.893 \times e\ 1.5271 - 4.808 \times e\ 1.3889$ (3) The goodness of fit of the model is 0.9701, and the mean square loss value is 1.23×10^{-2}. To further verify overfitting, Goodness of fit R^2 and mean square loss in Table 7 are used to judge the quality of results. The maximum value ofR^2 is 1, and the closer the value of R^2 is to 1, the betterthe regression line fits the observed value. Conversely, the smaller the value of R^2, the worse the regression line fits the observed value. Among them, the goodness of fit $R^2$of this model is 0.9800, and the mean square loss value is data with service time of 199.3 hours is brought into the model for testing. The predicted value of the obtained mass change value is 1.5094, and the error between the predicted value and the true value of 1.504 is small, further indicatingthe accuracy.

From Figure 10(a), it can be said that the mass loss curve during the oxidation stage corresponds well with the

diffusion control. However, there is a small deviation in predicting the mass loss during the oxidation stage with reaction control in the initial phase. This is because reactioncontrol should follow a linear equation.

To demonstrate the versatility of the proposed two- dimensional oxidation kinetics model for different types ofcomposite materials, a similar expression was further de- veloped to depict the relationship between the mass changeand service time of 3D SiC/SiC composite materials after oxidation in a $P_{H_2}O$:O_2:Ar = 21 : 21 : 58kPa environment.

Relationship model between mass change andservice time of 3D SiC/SiC in a $P_{H_2}O : O_2 : Ar = 21 : 21 : 58kPa$ ***environment***

We utilized the initial model architecture of Eq.(2) withthe specified parameter settings provided in Table 6 to solvethe relationship between the mass change and service time

of 3D SiC/SiC after oxidation at $P_{H_2}O$:O_2:Ar = 21 : 21 : 58kPa environment and 1100°C. The parameter values of

the model can be obtained as shown in Table 7, which can be carried into Eq.(2) to obtain: The model has a satisfying goodness of fit value of

0.99 and a mean square loss value of 2 × 10^{-3}. To further verify overfitting, data with a service time of 4.904 hours was introduced into the model. The predicted value ofthe obtained quality change value is 0.0314, and the error between the predicted value and the true value of 0.03077 issmall, further confirming accuracy.

Figure 10(b) indicates that the model effectively cap-tures the relationship between the mass change of 3D SiC/SiC composite material after oxidation at 1100°C and $P_{H_2}O$:O_2:Ar = 21 : 21 : 58kPa environment and its service time.

After deriving the expression for the relationship between the mass change and service time of 3D SiC/SiC

composite materials after oxidation at $P_{H_2}O$:O_2:Ar = 21 : 21 : 58kPa environment and 1100°C, we further employed

Eq.(2) to fit the relationship between the mass change and service time at temperatures of 1000°C, 1100°C,1200°C, 1300°C, 1400°C, and 1500°C. Table 7 presents the pre- dicted values of model parameters, the goodness of fit values of the model, and the mean square loss function values $y(t) = 0.04 \times (t-11.08)\ 2$

$2.07 + 0.04 \times e(t-6.91)\ \ 2\ 4.44$

(5) at these temperatures. These results, combined with the

experimental data from Figure 10(b) demonstrate that the model fitting effectively captures the relationship between mass change of 3D SiC/SiC composites after oxidation in a

$P_{H_2}O$:O_2:Ar = 21 : 21 : 58kPa environment and service time.

This section focuses on the development of a two- dimensional oxidation kinetics model for SiC_f /SiC. The model accurately represents the correlation between me- chanical performance parameters and service time of 2D SiC/BN/SiC-B_4C and 3D SiC/SiC composites. Moreover, the model architecture appears suitable for use within a specific temperature range.

Three-dimensional oxidation kinetics modelfor SiC_f/SiC

In this section, the main objective is to develop a three-dimensional oxidation kinetics model for SiC_f/SiC that can effectively analyze the correlation between mechanicalproperty parameters, service time, and service temperature after oxidation in various environments. Two steps solve the initial structure of the model and the determination of unknown parameters, as well as model adjustment based on experimental data. resulting in $p_1 = 1.894 \times 10^{-8}$, $p_2 = 7.155 \times 10^{-5}$,

$p_3 = -0.08742$, p_4 = 34.81. The reconstruction error of the model is 1.277 × 10^{-3}, indicating that the polynomial function can accurately fit the relationship between a_1 and.

According to the relationship expression between a_1 and T , the corresponding relation is plotted in Figure 11, confirming the accuracy of the selected polynomial approx-imation.

Similarly, it has been found through testing that the relationships between a_2, b_1, and b_2 with temperature also follow polynomial functions as shown in Figure 11. Inthe case of c_1 and c_1, there is no direct relationship with temperature, indicating that they may be influenced by otherfactors such as the type of material. Therefore, they are currently disregarded.

Finally, by substituting the values of a_1, a_2, b_1, and

Table 9: Predictive values of 3D SiC/SiC composite material model parameters.

Environment	Model parameters							
$P_{H_2O}: O_2: Ar = 21 : 21 : 58$kPa	P_1 4.4736	P_2 -0.6747	P_3 -0.2557	P_4 5.7710	P_5 5.9697	P_6 6.9773	P_7 -9.9377	P_8 -3.6506
	P_9 -0.4641	P_{10} -5.7583	P_{11} 6.8424	P_{12} 10.0167	P_{13} -13.7337			
$P_{H_2O}: O_2: Ar = 14 : 8: 78$kPa	P_1 1.6673	P_2 -5.0126	P_3 2.6175	P_4 4.2476	P_5 0.5642	P_6 4.7362	P_7 -1.7460	P_8 2.8732
	P_9 3.0824	P_{10} -2.5671	P_{11} -3.9636	P_{12} -0.5690	P_{13} 4.5893	P_{14} 1.6817	P_{15} -3.3090	
Air	P_1 0.3356	P_2 1.1536	P_3 0.0591	P_4 -2.6083	P_5 2.5055	P_6 -3.2702	P_7 5.3262	P_8 -2.0571
	P_9 1.1767	P_{10} -3.1350	P_{11} 3.4661	P_{12} 0.4553	P_{13} 4.0247			

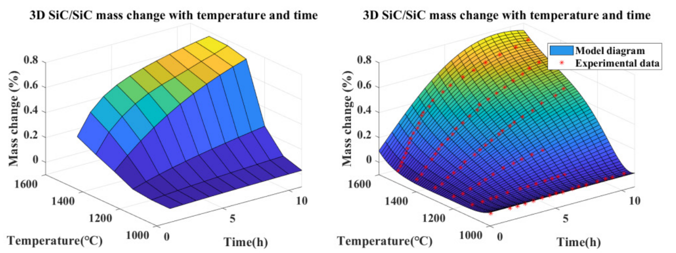

Figure 12: Proposed model and BPNN approximation of 3D SiC/SiC under $P_{H2O:O2:Ar}$ = 21: 21: 58kPa environment. a) BPNN. b) Proposed model.

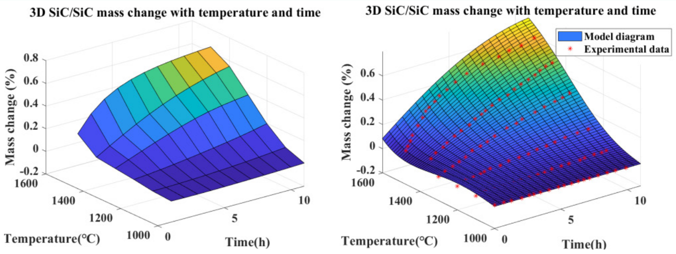

Figure 13: Proposed model and BPNN approximation of 3D SiC/SiC under $P_{H^2O:O2:Ar}$ = 14 : 8 : 78kPa environment. a) BPNN. b) Proposed model.

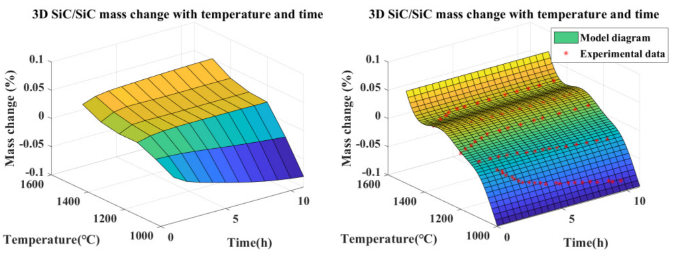

Figure 14: Model and BPNN approximation of 3D SiC/SiC under air environment. a) BPNN. b) Proposed model.

b_2, the relationship between mass change after oxidationin a environment and service time, as well as service temperature can be modified as follows:

$y(t,T) = (p_1 \times T^3 + p_2 \times T^2 + p_3 \times T + p_4)$

$-[(p5\times t-(p6\times T+p7))]^2 \times eRT(8)$ Initial architecture for the SiC_f ⁄ SiC composite material $+ (p_8 \times T^2 + p_9 \times T + p_{10}) - [(p11\times t-(p12\times T+p13))]^2$ he parameter prediction model of the two-dimensional $\times eRT$ oxidation kinetics model for SiC_f/SiC primarily reflects the correlation between mechanical property parameters and the service time after oxidation in various environments. Toexpand the model into a three-dimensional framework, the temperature variable is incorporated. According to Table 7, the relationship between theperformance parameters of strength of materials and the ser-vice time of 3D SiC/SiC composites after high-temperatureoxidation in different environments was calculated in Sec- tion 3.2. The findings indicated that the initial structure of the model remained the same at temperatures of 1000°C, 1100°C, 1200°C, 1300°C, 1400°C, and 1500°C. However, the final values of the six parameters (a_1, b_1, c_1, a_2, b_2 and c_2) varied. Therefore, we make a hypothesis that some of these parameters are not constants but rather variables dependent on temperature:

$$a_1 = f(T, \theta) \quad (6)$$

3D oxidation kinetic model of SiC_f ⁄ SiC

After obtaining the model describing the relationship between the mechanical properties of 2D SiC/SiC compos-ite materials after oxidation in various environments and their service time and temperature, the method described inSection 3.1 is employed to predict the unknown parametersof the model.

Based on the parameter estimation and the settings detailed in Section 3.1 and Table 8 , optimization algorithmcan be utilized to obtain $p_1 - p_{13}$ for the relationship expression between the mass variation of 3D SiC/SiC in a

$P_{H_2}O{:}O2{:}Ar = 21:21:58$kPa environment and its service time and temperature. The values of these parameters are presented in Table 9 and can be substituted into the final expression of the model:

$y(t, T) = (4.4736 \times T^3 - 0.6747 \times T^2 - 0.2557 \times T$ _ $[(5.9697\times t-(-6.9773\times T+9.9377))]^2$

where T represents temperature and θ is an unknown $+ 5.771) \times eRT(9)$ parameter. Based on Table 7, a data set is created for a_1 and the $+ (-3.6506 \times T^2 - 0.4641 \times T - 5.7587)$

$-[\underline{(6.8424\times t-(10.0167\times T-13.7337))}]^2$ corresponding temperature T. Temperature is considered asthe independent variable, while a_1 is the dependent variable. $\times eRT$Upon analyzing and testing the data patterns, it is postulatedthat the relationship between a_1 and temperature T can be represented by a polynomial function: The model has a predicted parameter error of 4.8 $\times 10^{-3}$. To check overfitting, three-dimensional plots correspondingto the model's expressions are generated and compared with $a_1(T) = p_1\times T^3 + p_2\times T^2 + p_3\times T + p_4(7)$ the neural network.

Figure 12 represents the neural network fitting on the According to Section 3.1, the parameter values of themodel were obtained through nonlinear least squares fitting left (a) and model on the right (b) for the mass variationof 3D SiC/SiC in a $P_{H_2}O{:}O2{:}Ar = 21 : 21 : 58$kPa environment. It can be observed that the model and the neural network exhibit a consistent fitting trend, effecti vely reflecting the mass variation of 3D SiC/SiC with respect totemperature and time. Additionally, the model graph shows that experimental data are well covered, further confirmingthe rationality and accuracy.

To demonstrate the applicability of the 3D SiC/SiC oxidation kinetics model to different environments, further expressions are constructed for the relationship between mass variation, service time, and service temperature of 3D SiC/SiC in two specific environments: $P_{H_2}O{:}O2{:}Ar = 14:8:78$kPa environment and air environment. Similarly, the relationship expression between mass variation, service time, and service temperature of 3D SiC/SiC in a $P_{H_2}O{:}O2{:}Ar = 14 : 8 : 78$kPa environment is proposed: $y(t,T) = (p_1\times T^4 + p_2 T^3 + p_3$

$\times T^2$ respect to temperature and time. Additionally, it can be seen from Figure 13(b) that all the experimental data points are well covered, further confirming the rationality and $+ p_4 \times T + p_5) \times e -[(p6\times t-(p7\times T+p8))]2\ RT$ (10) accuracy of the model. Similarly, the expression for the relationship between $+ (p_9 \times T^3 + p_{10} \times T^2 + p_{11} \times T + p_{12}) -[(p13\times t-(p14\times T+p15))]2$ the mass change in an air environment and the service time and service temperature is also postulated as follows: $\times eRT$ According to Section 3.1, and considering the parameter settings provided in Table 8, the unknown parameters $p_1 - y(t, T) = (p_1 \times T^3 + p_2 \times T^2 + p_3 \times T + p_4)$

$-[(p5\times t-(p6\times T+p7))]2\ p_{15}$ for the relationship expression between mass variation, $\times eRT$(12) service time, and service temperature of 3D SiC/SiC in the wet oxygen environment of $P_{H_2O}:O_2:Ar = 14 : 8 : 78$kPa $+ (p_8 \times T^2 + p_9 \times T + p_{10})$

$-[(p11\times t-(p12\times T+p13))]2$ can be obtained, as shown in Table 9. Substituting these values is (10) yields the final expression: $\times eRTy(t, T) = (1.667 \times T^4 - 5.0126 \times T^3 + 2.6175 \times T^2 + 4.2476 \times T + 0.5742) -[\underline{(4.7362\times t-(-1.746\times T+2.8732))}]2$ *According to the method and procedure for solving the unknown parameters of the model described in section 3.1, and considering the parameter settings in Table 8, the values of the unknown parameters* $p_1 - p_{13}$ can be identified through $\times eRT$(11) optimization. The obtained values of $p_1 - p_{13}$ are shown in $+ (3.0824 \times T^3 - 2.5671 \times T^2 + -3.9636 -[\underline{(4.5893\times t-(1.6817\times T-3.3090))}]2$ Table 9. Substituting these values into the model, the final expression is: $\times T - 5.690) \times eRTy(t, T) = (0.3356 \times T^3 + 1.1536 \times T^2 + 0.0591$ The predicted error of the model parameters is $3.1 \times -[\underline{(2.5055\times t-(-3.2702\times T+5.3262))}]2$ (13) 10^{-3}. To further check for overfitting, three-dimensional $\times T - 2.6083) \times eRT$ plots are generated based on the given equations. A comparison analysis is then performed between the model's plots and the plots obtained from the neural network fitting to evaluate the rationality and accuracy of the model.

Figure 13(a) shows the BPNN approximation, while Figure 13(b) illustrates the model of the mass variation of

3D SiC/SiC with temperature and time in a $P_{H_2O}:O_2:Ar = 14 : 8 : 78$kPa environment. By comparing the plot

with the neural network, it can be observed that the trend of Figure 13(b) is consistent with that of Figure 13(a), accurately reflecting the mass change of 3D SiC/SiC with $+ (-2.0571 \times T^2 + 1.1767 \times T + 3.1350)$

The model has a prediction error of 2.8×10^{-3}. To further check for overfitting, we generate three-dimensional plots and compare them with the neural network fitting images. This analysis will provide further insights into the rationality and accuracy of the model.

Figure 14(a) illustrates the fitting of the BPNN, while Figure 14(b) presents the model that depicts the mass variation of 3D SiC/SiC with respect to temperature and time in air environment. Upon comparing Figure 14(a)

time changes. Moreover, Figure 14(b) illustrates that experimental data are well encompassed, further confirming the rationality of the model.

This section primarily focuses on the phenomenon of quality change in 3D SiC/SiC composite materials. While physical factors like temperature and gas flow may exert some influence on the composite materials, their effects are fundamentally rooted in chemical reactions.

Chemical reactions typically assume control in the initial stage, but gradually transition to diffusion control over time. This transition is influenced by the oxidizing atmosphere, which triggers material oxidation, with the resulting oxide film serving as a barrier to further oxidation. The developed oxidation kinetics model accurately captures this change process in 3D SiC/SiC composite materials under the influence of multi-field coupling environments. By capturing the quality change resulting from the combination of multiple physical fields, the model offers a deeper understanding of the underlying mechanism of this change. In summary, the proposed oxidation kinetics model for SiCf/SiC accurately represents the correlation between mechanical properties and their degradation over time and at varying temperatures. Furthermore, the model can be effec-

tively applied in three different environments: $P_{H_2O}:O_2:Ar = 21 : 21 : 58$kPa, $P_{H_2O}:O_2:Ar = 14 : 8 : 78$kPa and air.

Conclusions and discussion

This study proposes an approach combining experimental methods and data analysis to investigate the effects of temperature, time, and atmosphere on the mechanical properties of SiC_f/SiC. By employing BPNN, we accurately assess the influence of these factors on the mechanical properties based on experimental data. Results indicate that the neural network performs better than conventional data fitting methods, especially when the training data is limited.

Moreover, the reconstructed curves obtained through the neural network not only reflect the direct impact of temperature and time on the mechanical properties of SiC_f/SiC composites but also allow reliable predictions at design points. Additionally, we construct a SiC_f/SiC composite material oxidation kinetics model using Gaussian functions and parameter optimization methods. This model accurately represents the relationship between the mechanical property parameters of SiC_f/SiC composites after high-temperature oxidation in different environments and their service time. It can be further extended to three dimensions to accurately represent the relationship between the mechanical property parameters, service time, and service temperature.

There are still certain aspects that require attention.

Firstly, while the mechanical property prediction and oxidation kinetic models of SiC_f/SiC have been supported by existing evidence, they have yet to be substantiated through specific experimental verification. Secondly, the oxidation kinetic model lacks a clear physical interpretation, which may pose challenges in comprehension. Lastly, there is no discussion regarding the applicability of the oxidation kinetics model in predicting the mechanical properties of other material types, potentially restricting its practical utility.

Future research will focus on addressing these three issues and continue to use machine learning methods and modeling theory to establish a robust SiC_f/SiC strength model. This model will contribute to a comprehensive analysis of the macroscopic mechanical properties of SiC_f/SiC and is expected to improve the accuracy and practicality. We will verify the accuracy and applicability of the model through experiments, further explore its physical meaning and universality, and aim to provide more comprehensive and detailed guidance for the performance re-

References

1. Sha JS, Dai JX, Zhan YF. Application research progress of fiber toughened high temperature ceramic matrix composite (c − f, sicf /sic) (in chinese). Aviat Manuf Technol. 2017; 66: 16-32.

2. Wang ZW, Zhang J, Fang DG. Research progress on the effect of interface layer on the mechanical properties of fiber reinforced ceramic matrix composite (in chinese). Equip Environ Eng. 2020; 17: 77-89.

3. Cheng LF, Luan XG, Zhang LT. Simulation of service behavior of ultra high temperature structural composite materials-theory and methods (in Chinese). Chemical Industry Press. 2203.

4. Wu SJ, Cheng LF, Zhang LT. Oxidation behavior of 3d hi-nicalon/sic composite exposed in wet and simulated air environments. Corros Sci. 2013; 66: 111-7.

5. Labrugère C, Guillaumat L, Guette A, Naslain R. Effect of ageing treatments at high temperatures on the microstructure and mechanical behaviour of 2d nicalon /c/sic composites. 2: Ageing under co and influence of a sic seal-coating. J Eur Ceram Soc. 1997; 17: 641-57.

6. Darzens S, Chermant J-L, Vicens J, Sangleboeuf J-C. Understanding of the creep behavior of SiCf–SiBC composites. Scr Mater. 2002; 47: 433-9.

7. Kim TT, Mall S, Zawada LP, Jefferson G. Simultaneous fatigue and combustion exposure of a sic/sic ceramic matrix composite. J Compos Mater. 2010; 44: 2991-3016.

8. Li LB. Damage development and lifetime prediction of fiber-reinforced ceramic-matrix composites subjected to cyclic loading at 1200◦c in vacuum, inert and oxidative atmospheres. Aerosp Sci Technol. 2019; 86: 613-29.

9. Wang X, Wang KJ, Bai H. Creep properties and damage mechanisms of 2d sicf ⁄sic through chemical vapor infiltration (in chinese). J Inorg Mater. 2020; 35: 817-21.

10. Xingang L, YunHai Z, Xiaohu. Degradation mechanisms of a self-healing sicf ⁄bni⁄[sic–b4c]m composite at high temperature under different oxidizing atmospheres. J Eur Ceram Soc. 2018; 38.

11. Gao XG, Han D, Song YD. ynamic strength design methods of ceramic matrix composite: research status and prospects (in chinese). J Mech Eng. 2021; 57: 235-47.

12. Xiguang G, Long L, Yingdong S. A temperature-dependent constitutive model for fiber-reinforced ceramic matrix composites and structural stress analysis. Int J Damage Mech. 2014; 23: 507-22.

13. Zhang S, Gao X, Han X, Duan H, Song Y, Song Ying- dong. Prediction of strength and constitutive response of sic/sic composites considering fiber failure. Composites. 2019; 163: 252-9.

14. Chen BM. A and C Qinghui Liu B. Multi-scale modelling of progressive damage and failure behaviour of 2d woven sic/sic composites. Ceram Int. 2021.

15. Anna M, Piotr B, Balaji R. Diffuse manifold learning of the geometry of woven reinforcements in composites. C R Mec Page S1631072118300779. 2018.

16. Anna M, Philippe C, Francois T, Adrien J, Maire E, Breitkopf P. Stochastic characterization of textile reinforcements in composites based on x-ray microtomographic scans. Compos Struct. 2019; 224: 111031.

17. Georgios K, Koumoulos Elias P, Charitidis Costas A. Classification of mechanism of reinforcement in the fiber-matrix interface: application of machine learning on nanoindentation data. Mater Des. 2020: 108705.

18. Laban O, Gowid S, Mahdi E, Musharavati F. Experimental investigation and artificial intelligence- based modeling of the residual impact damage effect on the crashworthiness of braided carbon/Kevlar tubes. Compos Struct. 2020; 243: 112247.

19. Trevor S, Kaan I, Pearl L-S. Application of artificial neural networks to predict fibre orientation in long fibre compression moulded composite materials. Compos Sci Technol. 2020; 190: 108034.

20. Anna M, Thuy V-PD, Tri NM, Nghiem NC, Piotr B, Franois T. Automated identification of defect morphology and spatial distribution in woven composites. Multidisciplinary digital publishing institute. 2020; 4.

21. Navid Z, Johannes R, Reza V. Theory-guided machine learning for damage characterization of composites. Com- posite Structures. 2020; 246: 112407.

22. Tao C, Zhang C, Ji H, Qiu J. Application of neural network to model stiffness degradation for composite laminates under cyclic loadings. Compos Sci Technol. 2021; 203: 108573.

23. Xiao M, Chao Z, Coelho RF, Tian S. Investigation of classification and anomalies based on machine learning methods applied to large scale building information modeling. Appl Sci. 2022; 12: 6382.

24. Szklarek K, Gajewski J. Optimisation of the thin-walled composite structures in terms of critical buckling force. Materials (Basel). 2020; 13: 3881.

25. Chen C-T, Gu Grace X. Generative deep neural networks for inverse materials design using back propagation and active learning. Adv Sci. 2020; 7: 1902607.

26. Mao Y, He Q, Zhao X. Designing complex architectured materials with generative adversarial networks. Sci Adv. 2020; 6: eaaz4169.

27. Khatir S, Tiachacht S, Thanh C, Bui TQ, Abdel Wahab M. Damage assessment in composite laminates using ann-pso-iga and Cornwell indicator. Compos Struct. 2019; 230: 111509.

28. Zimo W, Pawan D, Faissal C, Behrouz T, Tai Bruce L, Mohamed EM, et al. Bidirectional gated recurrent deep learning neural networks for smart acoustic emission sensing of natural fiber–reinforced polymer composite machining process. Smart Sustain Manuf Syst. 2020; 4: 179-98.

29. Asif K, Soo KH. Classification and prediction of multidamages in smart composite laminates using discriminant analysis. Mech Adv Mater Struct. 2020: 1-11.

30. Ji X, Dai S. Application of bp neural network in glass defect identification. Softw Guide. 2019: 1-5.

31. Liu D, Li S, Fu Q, Liu C. Comprehensive evaluation method of groundwater quality based on bp network optimized by krill herd algorithm. Trans Chin Soc Agric Mach. 2018; 49: 275-84.

32. Hai XH. Study on the oxidation and tensile creep properties of 2d self-healing sic/sic materials in high-temperature water oxygen environment (in chinese) [Master's thesis]. Xi'an: Northwestern Polytechnical University. 2017.

33. Wu SD. Thermochemistry environmental behavior of 3D SiC/SiC composites [doctoral dissertation] (in chinese) [PhD thesis], North- western Polytechnical University, Xi'an. 2006.

34. Xiang H, Cheng L, Wei X, Luan X. Modelling of oxidation Kinetics of c/sic composites based on factorization method. Guisuanyan Xuebao (J Chin Ceram Soc)(China). 2004; 32: 1335-40.

35. Litofsky J, Viswanathan R. Introduction to computational chemistry: teaching huckel molecular orbital theory using an excel workbook for matrix diagonalization. J Chem Educ. 2015; 92: 291-5.

36. David C, cramer Cj. Essentials of computational chemistry: theories and models. Theor Chem Acc. 2002; 108: 367-8.